e-ISSN: 2550-164X

Available online at
https://jmeche.uitm.edu.my/

Journal of Mechanical Engineering 23(1) 2026, 212 – 237.

Journal of Mechanical Engineering

An ANN-Based Fuel Injection Strategy for Green Hydrogen-Enriched Advanced CRDI Engine: The Paradigm Approach of NSGA-II and TOPSIS

P. Ajay Goud[1*], Mohammad Sikindar Baba[1]

[1]*Department of Mechanical Engineering, School of Engineering, Anurag University, Hyderabad, India*

ARTICLE INFO

Article history:
Received 03 September 2025
Revised 19 December 2025
Accepted 28 December 2025
Online first
Published 15 January 2026

Keywords:
Hydrogen
Palm kernel methyl ester
Combustion strategy
Emission control

DOI:
10.24191/jmeche.v23i1.8763

ABSTRACT

This study investigates the influence of fuel injection pressure and timing on the performance, combustion, and emission characteristics of a single-cylinder, 1500 rpm common rail direct injection (CRDI) diesel engine fueled with a diesel–biodiesel blend containing 20% palm kernel methyl ester and 80% diesel, enriched with hydrogen at a flow rate of 10 LPM (PKME20H10). The objective is to enhance engine efficiency and emission control through a green hydrogen–biodiesel strategy. Artificial Neural Network (ANN) models were developed to predict engine responses, and optimization was achieved using the hybrid Non-Dominated Sorting Genetic Algorithm II (NSGA-II) coupled with the Technique for Order Preference by Similarity to Ideal Solution (TOPSIS). Experimental and computational analyses revealed that the optimal combination of an injection timing of 25° before top dead center (BTDC) and an injection pressure of 512 bar achieved a brake thermal efficiency (BTE) of 30.1%, a brake specific fuel consumption (BSFC) of 0.123 kg/kWh, and substantial reductions in emissions. Carbon monoxide emissions decreased by 10%, unburnt hydrocarbon emissions decreased by 45%, and smoke opacity decreased by 17%. The study demonstrates that hydrogen enrichment in biodiesel improves combustion quality and engine sustainability, offering a viable pathway for low-carbon automotive energy systems.

INTRODUCTION

The global energy scenario is rapidly evolving due to concerns over fossil fuel depletion, rising greenhouse gas emissions, and the growing demand for cleaner and renewable energy sources. The transportation sector, which heavily depends on diesel and petrol, is one of the major contributors to air pollution and carbon emissions (Prabhu et al., 2023a; Shen et al., 2023; Praveenkumar et al., 2023). This dependence has prompted significant research efforts toward developing sustainable alternatives that can be directly utilized

[1*] Corresponding author. *E-mail address*: ajaypodicheti@gmail.com
https://doi.org/10.24191/jmeche.v23i1.8763

in existing compression ignition (CI) engines without extensive modification. Among these alternatives, biodiesel has gained substantial attention because of its renewability, non-toxic nature, high biodegradability, and lower emission footprint (Anand & Debbarma, 2024; Nithya et al., 2023; Prabhu et al., 2023b).

Biodiesel is typically derived from vegetable oils or animal fats through transesterification, resulting in fatty acid methyl esters (FAME) suitable for CI engine operation. Several studies have demonstrated that biodiesel can partially replace conventional diesel without compromising basic engine performance. B20 (20% biodiesel and 80% diesel) blends demonstrate brake thermal efficiency (BTE) comparable to diesel, while significantly reducing hydrocarbon (HC), carbon monoxide (CO), and smoke emissions. Studies on palm, karanja, jatropha, soybean, and mahua biodiesels further confirm that inherent oxygen content enhances combustion efficiency and suppresses particulate formation (Anderson et al., 2023; Kumar & Choudhary, 2023; Mohite et al., 2024a). However, biodiesel exhibits certain limitations such as higher viscosity, lower volatility, and reduced calorific value, which can negatively influence atomization and fuel–air mixing at low loads (Nibin et al., 2024; Gültekin et al., 2024). These drawbacks often result in incomplete combustion and slightly higher fuel consumption compared to diesel (Mohite et al., 2024b; Panda et al., 2025).

To address these performance gaps, researchers have explored hydrogen enrichment as a complementary approach to improve biodiesel combustion. Hydrogen, being a carbon-free energy carrier, possesses a high flame speed, wide flammability limits, and excellent diffusivity (Kanth et al., 2020; Akcay et al., 2020; Jamrozik et al., 2020). These properties promote faster and cleaner combustion when introduced into the intake manifold or directly into the cylinder of a CI engine. Hydrogen supplementation has been found to enhance BTE, reduce HC and CO emissions, and improve the heat release profile (Jabbr & Koylu, 2019; Santhosh & Kumar, 2021). Kanth et al. (2019) reported a 2.2% improvement in BTE and a 24% reduction in CO emissions when hydrogen was blended with biodiesel under dual-fuel conditions. Jabbr & Koylu (2021) showed that hydrogen addition in hydrogen–diesel mixtures reduced soot by 60%, while Akcay et al. (2021) observed higher in-cylinder pressure and improved combustion completeness in hydrogen-enriched waste-oil biodiesel. Similar studies by Sun et al. (2024) and Jia et al. (2024) concluded that moderate hydrogen flow rates (4 L/min - 10 L/min) enhanced engine performance and reduced emissions, though excessive enrichment caused NOx to rise due to higher combustion temperatures.

Hydrogen therefore, acts as an efficient supplementary fuel for biodiesel-powered engines, yet its optimal proportion and control parameters require precise calibration. The oxides of nitrogen (NOx)–efficiency trade-off remains a persistent challenge because increasing hydrogen concentration improves combustion efficiency but also elevates in-cylinder temperatures that accelerate NOx formation (Holman & Gajda, 1978; Debbarma et al., 2020). Hence, fine-tuning of injection pressure (IP) and injection timing (IT) is essential to balance combustion quality, emission characteristics, and fuel economy (Bhowmik et al., 2025; Vadlamudi et al., 2025). Injection timing determines the start of combustion and influences ignition delay, while injection pressure controls atomization and air–fuel mixing. Earlier injection tends to increase peak pressure and temperature, leading to improved BTE but higher NOx, whereas delayed injection may reduce thermal efficiency and increase CO and HC emissions. Similarly, higher injection pressure promotes finer spray formation and faster mixing but may also contribute to increased NOx at elevated loads (Seelam et al., 2022; Ramachander et al., 2021).

A review of recent literature highlights a clear research gap: although several studies have addressed biodiesel–hydrogen dual-fuel operation, very few have investigated the combined optimization of injection timing and pressure using a systematic multi-objective framework. Most prior studies focused on experimental variations of either fuel composition or injection parameters, neglecting their complex nonlinear interactions. Given that multiple engine responses such as brake thermal efficiency (BTE), brake specific fuel consumption (BSFC), NOx, smoke, and CO must be optimized simultaneously, classical

https://doi.org/10.24191/jmeche.v23i1.8763

methods alone are insufficient for deriving the best compromise solution. Consequently, advanced computational intelligence techniques have become indispensable in modern engine optimization.

Artificial Neural Networks (ANNs) have emerged as a powerful tool for modeling complex nonlinear relationships among engine input and output parameters. ANNs can accurately predict responses such as performance and emissions based on experimental datasets, minimizing the number of physical tests required. They have been effectively applied to simulate combustion behavior in diesel, biodiesel, and dual-fuel engines with high correlation accuracy (Vadlamudi et al., 2023a). However, prediction alone does not resolve the optimization challenge. Therefore, evolutionary algorithms, particularly the Non-Dominated Sorting Genetic Algorithm II (NSGA-II), are often employed for multi-objective optimization. NSGA-II can efficiently identify a set of Pareto-optimal solutions that represent the best trade-offs between conflicting objectives such as high efficiency and low emissions. Since NSGA-II produces multiple optimal solutions, decision-making techniques like the Technique for Order of Preference by Similarity to Ideal Solution (TOPSIS) are subsequently integrated to rank and select the most balanced configuration (Vadlamudi et al., 2023b; Santosh & Kumar, 2021).

The integration of ANN with NSGA-II and TOPSIS offers a robust hybrid framework that bridges the gap between experimental data and intelligent decision-making. ANN-based metamodels predict performance and emission responses under diverse injection settings, NSGA-II explores the optimization space, and TOPSIS identifies the most feasible solution. This combination ensures accurate prediction, efficient optimization, and systematic ranking of results, enabling data-driven improvements in fuel injection control strategies for hydrogen–biodiesel dual-fuel common rail direct injection (CRDI) engines. This study experimentally and computationally optimizes a CRDI engine using diesel–biodiesel blend containing 20% palm kernel methyl ester with 10 LPM hydrogen enrichment (PKME20H10), analyzing injection timing and pressure effects at 1500 rpm. The engine data are then used to train and validate ANN models, which are further coupled with NSGA-II and TOPSIS for identifying the best compromise configuration between thermal efficiency and emissions. The study aims to establish a reproducible methodology that integrates empirical experimentation with artificial intelligence-based multi-objective optimization. It is important to note that while the introduction previously mentioned long-term engine performance, economic viability, lifecycle assessment, and advanced real-time control systems, these aspects were not within the current experimental scope. The primary emphasis of this study is therefore limited to performance, combustion, and emission optimization of hydrogen–biodiesel blends under different injection strategies. The long-term and economic analyses are acknowledged as future research directions that will extend the present findings toward holistic sustainability assessment.

In summary, this study explores the effect of hydrogen enrichment and injection parameter variation on biodiesel fueled CRDI engine operation. It develops an intelligent ANN–NSGA-II–TOPSIS framework for optimal parameter selection, aiming to enhance energy efficiency, minimize pollutant emissions, and contribute to cleaner engine technologies aligned with global carbon neutrality goals.

EXPERIMENTAL SETUP AND PROCEDURE

Experiments used a single-cylinder CRDI diesel engine with eddy-current dynamometer; specifications, setup, as illustrated in Fig 1, and output uncertainty analyses are summarized in Tables 1 and 2.

Fuel blend preparation

The palm kernel methyl ester (PKME) used in this study was produced by transesterification of crude palm kernel oil with methanol and potassium hydroxide (KOH) under controlled temperature and agitation at Apex Innovations Laboratory, Pune (India), attaining > 98 % conversion. The purified biodiesel was blended with diesel to prepare PKME20 (20 % biodiesel + 80 % diesel). Table 3 shows the details of

https://doi.org/10.24191/jmeche.v23i1.8763

physicochemical properties of fuels used in the study. For hydrogen enrichment, compressed hydrogen (purity > 99.99 %) was supplied from a 250-bar cylinder through a pressure regulator, flame arrester, and flow-control valve. The flow rate was maintained at 10 L min^{-1} using a calibrated rotameter, forming the PKME20H10 mixture.

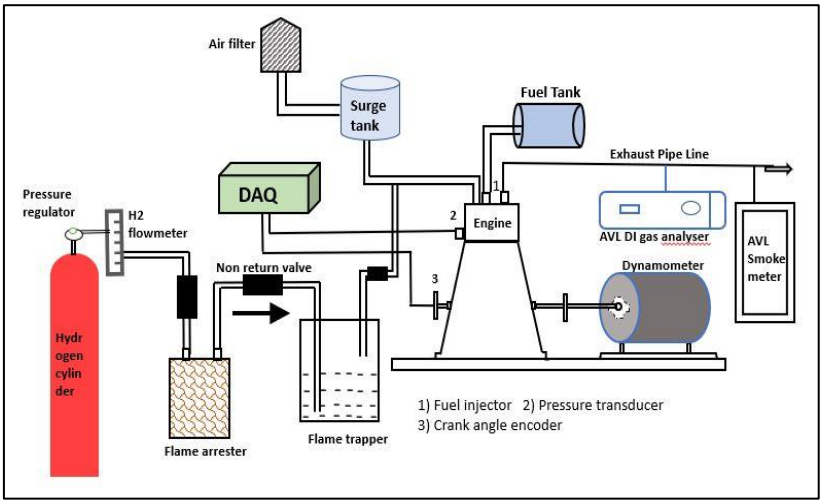

Fig. 1. Experimental setup.

Table 1. Engine specifications

Different parameters	Specifications
Model	APEX Cr.DI.
Rated power, dynamometer	5.2 (kW), Eddy current
Speed	1500 (rpm)
Compression ratio and cylinder bore	17.5:1 & 87.5 (mm)
Stroke (mm)	110

Table 2. Uncertainty parameters

Parameters	Accuracy and uncertainty (%)
Measured values	
Speed (rpm)	± 1 & ± 1.42
HC (ppm)	± 10 & ± 1.0
CO	± 0.01 & ± 0.5
NO_x (ppm)	± 10% & ± 1.52
Smoke opacity	± 1% & ± 2
Calculated values	
BTE	– & ± 0.8
BSFC	– & ± 0.25

https://doi.org/10.24191/jmeche.v23i1.8763

Table 3. Physicochemical properties of fuels used in the study

Fuel	Cetane number / Octane number	Density (kg/m³)	Viscosity (mm²/s)	Calorific value (MJ/kg)
Diesel	46	834	3.32	44.552
PKME100	51	886	4.66	42.255
PKME20	48	872	3.91	42.188
Hydrogen	130 (Octane number)	0.06	0.84	118.3

Test conditions and measurements

Experiments were conducted at a constant speed of 1500 rpm under six brake-power (BP) levels (1.0 – 3.5 kW). Injection pressures of 400, 500, and 600 bar and injection timings of 21°, 23°, and 25° CA bTDC were tested. A piezoelectric pressure transducer mounted on the cylinder head recorded in-cylinder pressure, and data acquisition was performed through a high-speed interface with LabVIEW software. K-type thermocouples measured intake-air, exhaust-gas, and lubricant temperatures. CO, CO_2, NOx, and HC were measured using an AVL five-gas analyzer, and smoke opacity was determined using an AVL 437 smoke meter. All instruments were calibrated prior to testing, and each point was recorded after 15 min of steady-state operation. The hydrogen line shown in Fig 2 consisted of a cylinder, flow meter, flame arrester, and non-return valve; manifold pressure was maintained at 2 bar to ensure uniform air-fuel mixing and operational safety.

Experimental protocol

Baseline data were first obtained with D100, followed by PKME20 and PKME20H10 under identical load and parameter conditions. Each test was repeated three times, and the average value was used for analysis. The measured parameters in-cylinder pressure, heat-release rate, and ignition delay were used to interpret the effect of injection timing and pressure on combustion, performance, and emissions.

Artificial neural network (ANN) methodology

ANN models predicted engine performance, combustion, and emissions using experimental hydrogen-biodiesel data. The network was trained and validated using MATLAB R2023b Neural Network Toolbox, following the feed-forward back-propagation algorithm.

Network configuration

A three-layer feed-forward architecture (input, hidden, and output layers) was employed.

- Input parameters: Load, injection pressure, injection timing, fuel type (D100, PKME20, PKME20H10), and hydrogen flow rate.
- Output parameters include BTE, BSFC, UHC, CO, smoke opacity, and NOx.

The log-sigmoid activation function was used in the hidden layer and the linear transfer function in the output layer. The network weights were optimized using the Levenberg–Marquardt (trainlm) back-propagation algorithm owing to its rapid convergence and stability in nonlinear mapping problems (Dahake et al., 2024; Pitchaiah et al., 2023).

Data division and training

The total dataset, comprising 162 experimental observations, was randomly divided into:

- Training set – 70 %,
- Validation set – 15 %, and

https://doi.org/10.24191/jmeche.v23i1.8763

- Testing set – 15 %.

During training, the algorithm iteratively minimized the Mean Squared Error (MSE) between predicted and experimental values until convergence. The performance of each developed model was evaluated using the statistical indices Mean Absolute Percentage Error (MAPE), Root Relative Squared Error (RRSE), and the correlation coefficient (R) as defined in Equations 1–3. Low MAPE/RRSE and high R values confirmed model accuracy (Liao et al., 2023).

Integration with optimization framework

The validated ANN models were integrated with NSGA-II for multi-objective optimization, while TOPSIS identified the most balanced solution from the Pareto set. This integrated framework allowed simultaneous optimization of efficiency and emission parameters, forming the methodological backbone of this research (Wang et al., 2023; Zeng et al., 2023).

RESULTS AND DISCUSSION

The optimization of injection time and injection pressure of a diesel-biodiesel blended fuel for a hydrogen-enriched engine is being showcased in the current research work. The discharge of the engine considered for the study is around 7 lpm to 13 lpm. In case of a hydrogen engine, the deviation of the brake thermal efficiency for varying brake power is illustrated in Fig 2(a). The brake thermal efficiency ascends with an ascending flow rate of hydrogen and vice versa, as observed from Fig 2(a). However, in the case of higher loads, the amount of NOx emitted is significantly higher for a rise in the flow rate of hydrogen (at 13 lpm), as shown in Fig 2(b). Henceforth, the flow rate of hydrogen was fixed at 10 lpm to obtain the required results by changing the parameters, viz., injection pressure and injection time.

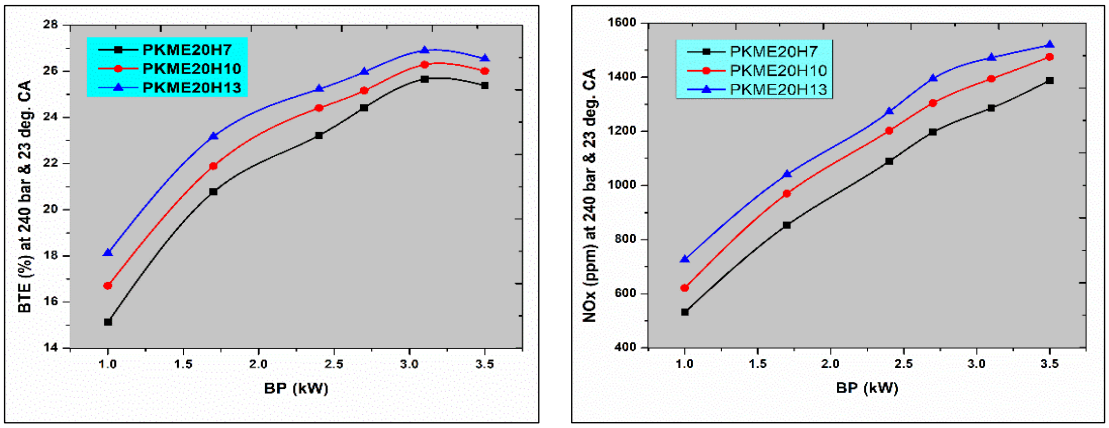

(a) (b)

Fig. 2. (a) Variation in BTE with different fuel and (b) variation in NOx of different fuel.

Energy share

The study explores pre-mixed lean combustion by analyzing the energy contribution of injected fuel. It found that hydrogen intake impact during combustion is minimal under varying PKME20 inputs, load, and injection parameters. Higher energy contributions from hydrogen in dual-fuel engines are controlled by increasing injection pressures and times, especially as PKME20 provides more energy at higher loads. Combining hydrogen with PKME20 increases energy share during combustion, particularly with injection

https://doi.org/10.24191/jmeche.v23i1.8763

pressures raised from 400 to 500 bar. At 600 bar, using a hydrogen-PKME20 blend lowers cylinder internal temperatures, preventing flame spread (Vadlamudi et al., 2025). This modulation of energy share in dual-fuel mode considers the energy ratio of primary to pilot fuel.

Table 4 shows variations of injection time and pressure for both Hydrogen and PKME20 at a discharge of 10 lpm or 0.05 kg/h of introducing hydrogen. For Hydrogen and PKME20, it was observed that, with the variation of injection pressure, energy shared with brake power varies too, as shown in Fig 3(a)-(b).

Table 4. Experimental matrix

Test fuels	FIT and IT
D100, PKME20, PKME20H10	21° CA bTDC, 23° CA bTDC, 25° CA bTDC 400, 500 & 600 bar

*FIT – Fuel Injection Timing (expressed in crank angle degrees before top dead center, ° CA bTDC)
*IT – Injection Timing / Injection Pressure variable pair, indicating the combined test parameter in which injection timing (° CA bTDC) and injection pressure (bar) were systematically varied to study their influence on performance and emissions.

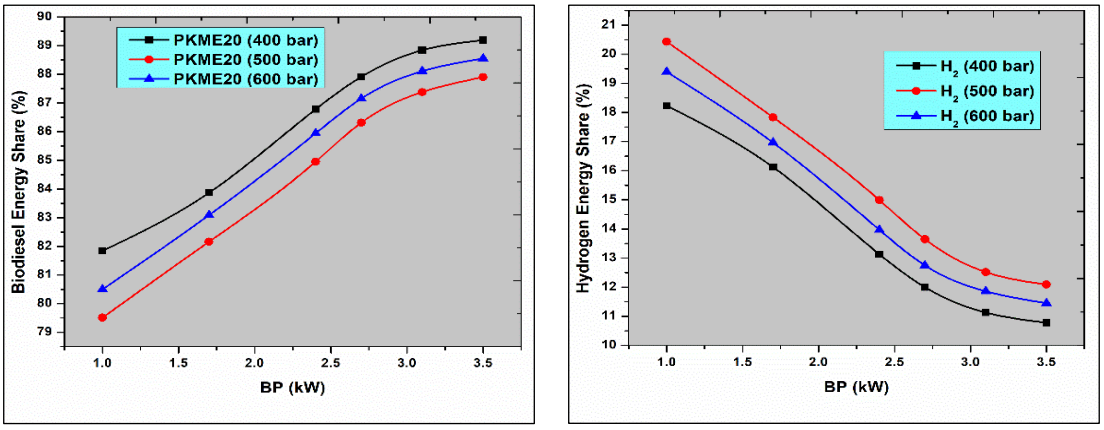

(a) (b)

Fig. 3. Energy shared with brake power (a) different fuel and (b) H_2 different IP.

Combustion characteristics

In-cylinder pressure

Changes in injection timing significantly impact cylinder pressure dynamics, as observed in Fig 4. Enhanced timing increases the pressure, raising the temperature and pressure around the top dead center. Early injection, initially inadequate for combustion support, necessitates additional fuel to increase chamber density and facilitate rapid combustion at a pre-mixture stage, elevating maximum pressure from 400 to 500 bar. PKME20H10 shows a 5.55% higher injection timing than diesel, reaching peak cylinder pressures around 72 bar at 500 bar injection pressure. Conversely, PKME20 has a 7.35% lower timing due to quicker ignition and better atomization. As pilot fuel ignites 1° - 3° before diesel and biodiesel, cylinder pressure escalates with increased hydrogen content. Higher pressures achieved by advancing the injection pressure from 500 to 600 bar result in finer atomization and reduced spray momentum, while quicker ignition from the premixed fuel leads to pressure improvements (Farooq et al., 2024; Panda et al., 2025; Seelam et al., 2022). However, the biodiesel blend shows weaker atomization due to higher viscosity and surface tension, impacting pressure behavior during the injection cycle at 21° CA bTDC (Nithya et al., 2023; Anderson et al., 2023; Isler-Kaya & Karaosmanoglu, 2023).

https://doi.org/10.24191/jmeche.v23i1.8763

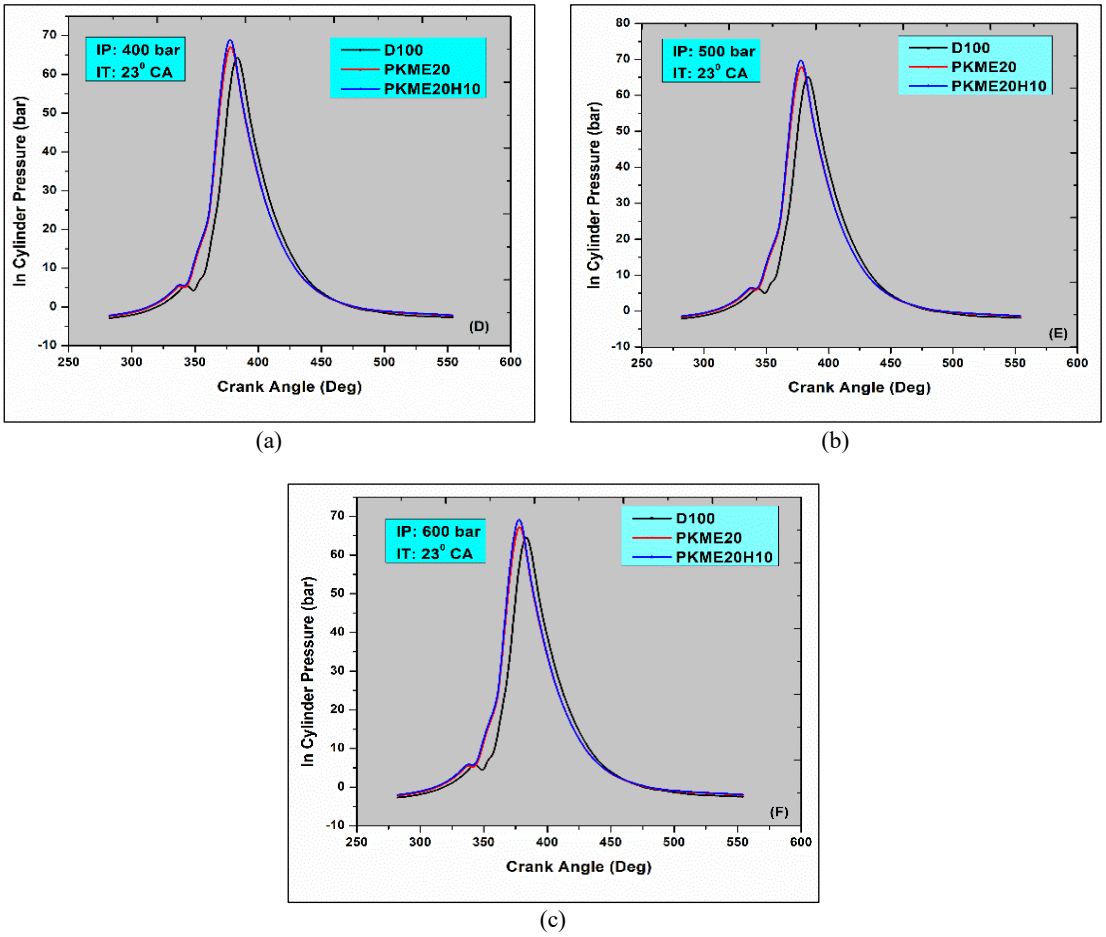

Fig. 4. In-cylinder pressure: (a) 400 bar, (b) 500 bar, and (c) 600 bar.

Heat release rate

Fig 5 showcases how different injection timings and pressures impact heat release in diesel engines with hydrogen-enhanced fuels, based on data averaged over 100 engine cycles. Heat release rate, crucial for diesel combustion prediction, adheres to the first law of thermodynamics (Santhosh & Kumar, 2021; Seelam et al., 2022; Ramachander et al., 2021). The PKME20 blend at 500 bar and 23° CA bTDC achieves a heat release rate of 44.21 J/CA, 10.45% lower than pure diesel. This is due to PKME20's higher latent heat, lower calorific value, and viscosity, leading to larger fuel droplets and less efficient vaporization at partial loads. However, at full load, higher cylinder temperatures break these droplets into smaller fragments, improving combustion. Hydrogen's impact varies; it leans the fuel mix at lower loads, reducing heat release, while at higher loads, it boosts peak heat due to its high diffusivity. PKME20H10 consistently exhibits the highest heat release across all settings, benefiting from advanced injection timings for better air-fuel mixing and combustion efficiency. Higher pressures enhance the mixture and maximize heat release, as seen in steeper slopes on the heat release rate curve, indicating extended combustion phases. Increased injection pressures create finer spray droplets, accelerating the air-fuel mixture and reducing combustion initiation time, especially for hydrogen and biodiesel blends burning earlier. These blends at 500 bar reach a maximum cylinder pressure of 56.5 J/CA, 20% higher than diesel, improving combustion but also posing challenges like fuel wall extinguishing (Loganathan et al., 2020; Akcay et al., 2021).

https://doi.org/10.24191/jmeche.v23i1.8763

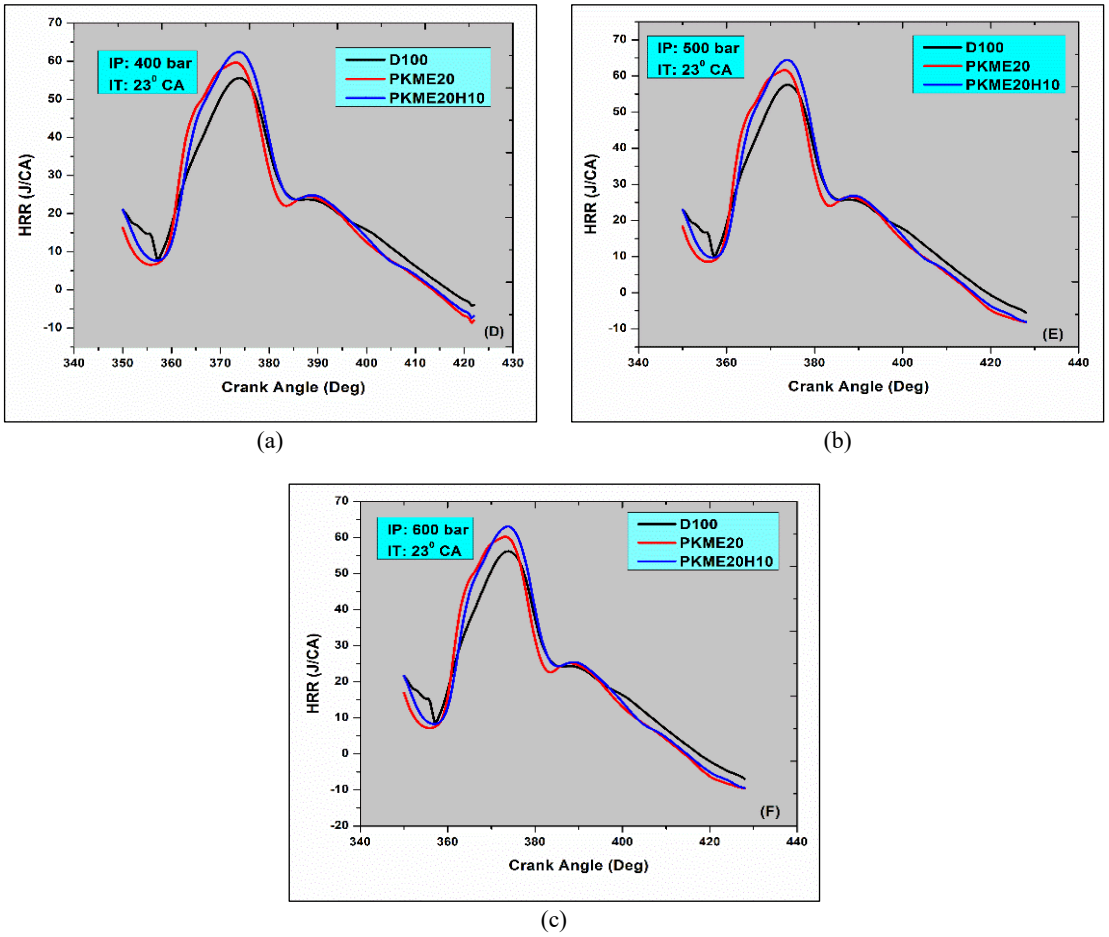

Fig. 5. Heat release rate (HRR): (a) 400 bar, (b) 500 bar, and (c) 600 bar.

Ignition delay

Fig 6 illustrates how engine load influences ignition delay across various fuels. Higher cylinder temperatures at increased loads reduce ignition delays. PKME20, with its higher oxygen content, mixes more readily than other fuels, resulting in a 20% shorter delay than diesel at high loads. Conversely, hydrogen's higher auto-ignition temperature prolongs mixing time, complicating engine starts. The higher cetane number of pilot fuels extends combustion duration, affecting cylinder temperature and auto-ignition (Seelam et al., 2022; Vadlamudi et al., 2023b). PKME20H10 shows a 25% reduction in ignition delay compared to neat diesel, highlighting faster combustion readiness at full load.

The present findings are consistent with previous observations by Akcay et al. (2021) and Jamrozik et al. (2020) who reported enhanced premixed combustion and increased cylinder pressure with hydrogen addition in diesel and biodiesel dual-fuel engines. In this study, PKME20H10 exhibited approximately 13% 15% higher peak in-cylinder pressure than D100 at 500 bar, which aligns with the 10% - 14% improvement reported by Kanth et al. (2020) for hydrogen-enriched honge biodiesel. This enhancement confirms the superior flame propagation and heat release characteristics of hydrogen-assisted combustion.

https://doi.org/10.24191/jmeche.v23i1.8763

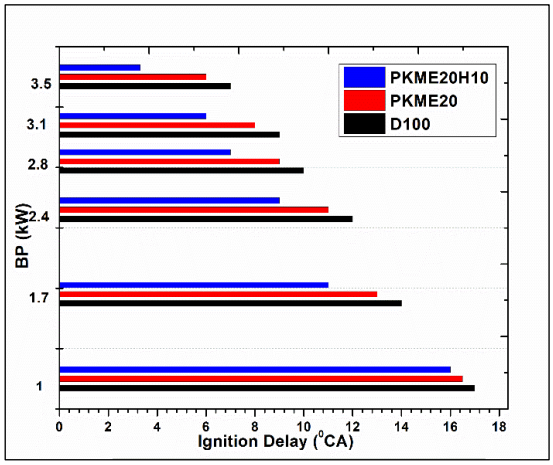

Fig. 6. Ignition delay.

Performance characteristics

Brake thermal efficiency

Fig 7 highlights the impact of injection timings and pressures on Brake Thermal Efficiency (BTE) for PKME20, diesel, and hydrogen blended PKME20 (PKME20H10). At 400 bar and 230 CA bTDC, BTE is recorded at 26% for PKME20 and 25.4% for diesel. Increased pressures and optimal mixing, achieved through better atomization, elevate BTE; at 500 bar and 230 CA bTDC, PKME20 shows a BTE of 25.71%, diesel at 26.78%, and PKME20H10 reaches 28%. These results underscore the role of precise injection timing and higher pressure in enhancing thermal efficiency by improving the air-fuel mixture and combustion quality. However, as pressure escalates to 600 bar, despite faster combustion due to higher calorific value and burning speed of hydrogen in PKME20H10, BTE decreases slightly due to the extended time required to build pressure and the effects of higher viscosity and surface tension under different engine conditions (Farooq et al., 2024; Nibin et al., 2024; Vadlamudi et al., 2023b).

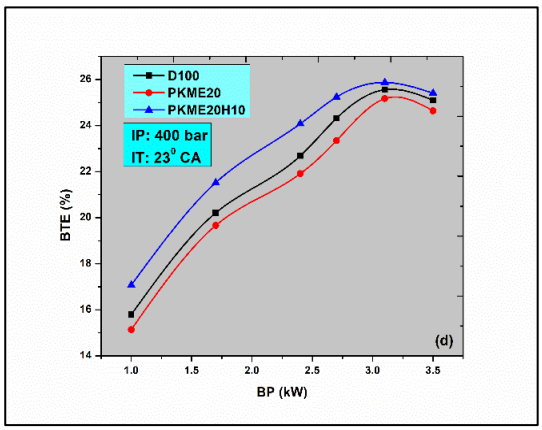

(a)

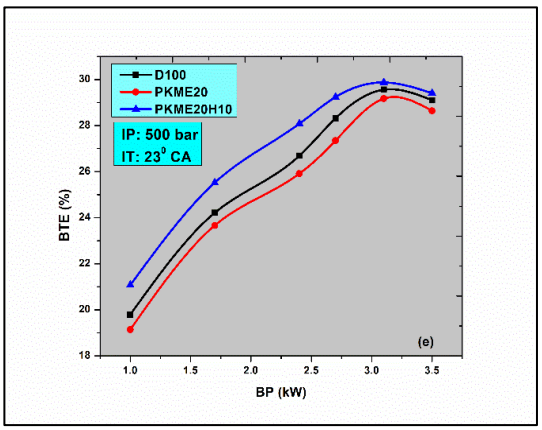

(b)

https://doi.org/10.24191/jmeche.v23i1.8763

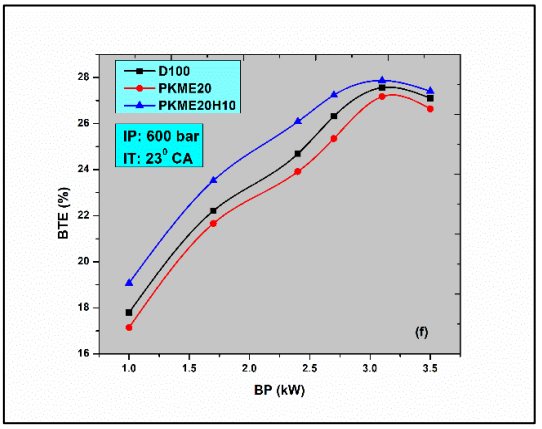

(c)

Fig. 7. Variation of brake thermal efficiency (BTE): (a) 400 bar, (b) 500 bar, and (c) 600 bar.

The BTE of PKME20H10 exceeded that of pure diesel by 4% - 5%, particularly at 500 bar and 23° CA bTDC, which reflects the synergistic combustion of biodiesel oxygen and hydrogen's high diffusivity. Similar results were reported by Tayari & Abedi (2019) and Mohite et al. (2024b), who observed 3% - 6% improvement in efficiency with microalgae- and algae-derived biodiesel–hydrogen blends. These comparisons affirm that the current PKME20H10 blend offers higher efficiency than both neat diesel and conventional biodiesel blends due to improved atomization and shorter ignition delay.

Brake specific fuel consumption

Brake-specific fuel consumption (BSFC) trends spanning injection timings and pressures are shown in Fig 8. As load increases, BSFC falls for all test fuels, regardless of injection timing or pressure. BSFC is 0.29 kg/kWh for the PKME20H10 version at 90% load, 23° CA bTDC injection timing, and 500 bar injection pressure. However, BSFC is 0.33 kg/kWh for PKME20 at the same load. Compared to diesel, PKME20H10 has a 6.45% lower BSFC and PKME20 a 6% higher one. Increased injection pressure improves air-fuel mixture efficiency, lowering BSFC in the PKME20H10 version. To compensate for PKME20H10's slower evaporation, fuel injection is increased. Hydrogen-rich fuels have lower BSFC due to higher flame speed, wider flammability range, and shorter quenching distance. BSFC improves when injection pressure hits 600 bar due to inefficient air-fuel diffusion. Injecting fuel at lower cylinder temperatures and changing the injection time from 23° to 25° CA bTDC reduces combustion efficiency and BSFC (Nithya et al., 2023; Runyon et al., 2024; Liao et al., 2023).

A comparative reduction of 6.4% in BSFC for PKME20H10 over D100 correlates well with the 5% - 7% reduction reported by Jabbr & Koylu (2019) for hydrogen-diesel dual-fuel engines. The improvement is attributed to hydrogen's rapid flame propagation and uniform energy release, confirming that the fuel blend used in the present study performs competitively with prior hydrogen-enriched biodiesel systems.

https://doi.org/10.24191/jmeche.v23i1.8763

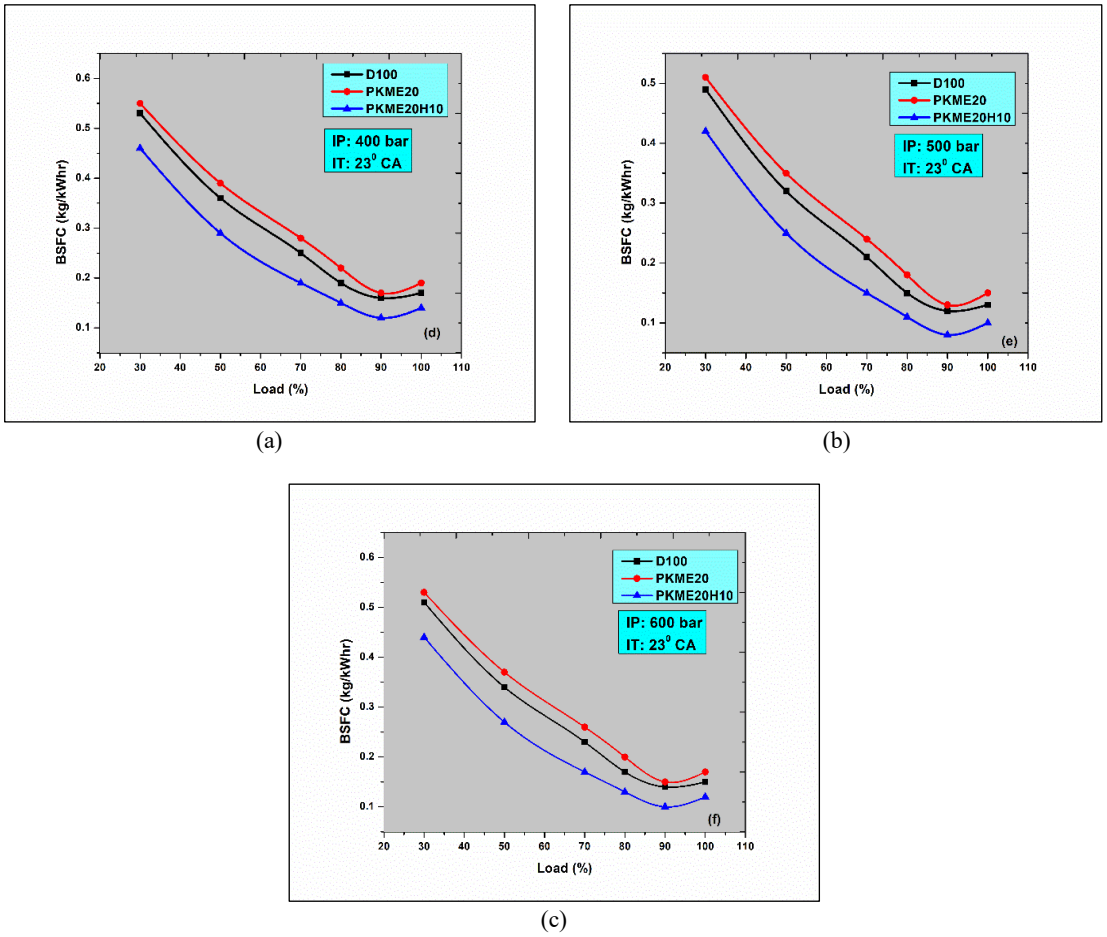

Fig. 8. Variation of brake-specific fuel consumption (BSFC): (a) 400 bar, (b) 500 bar, and (c) 600 bar.

Emission characteristics

Unburnt hydrocarbon emission

Fig 9 illustrates how injection timings and pressures influence unburnt hydrocarbon emissions using PKME20, diesel, and a hydrogen-biodiesel mix (PKME20H10). At 500 bar, optimal air-fuel mixing significantly lowers unburnt hydrocarbons, while at 600 bar, suboptimal combustion increases them. Advanced timing at lower pressures effectively reduces emissions; however, at pressures above 600 bar, emissions rise due to less efficient combustion. The addition of hydrogen, known for its higher calorific value and broad flammability range, consistently lowers unburnt hydrocarbons across all pressures. Enhanced injection timing improves combustion efficiency and reduces hydrocarbon emissions, with PKME20H10 and PKME20 showing 34 ppm and 40 ppm, respectively at 500 bar, significantly outperforming diesel (Vadlamudi et al., 2023a; Liao et al., 2023).

https://doi.org/10.24191/jmeche.v23i1.8763

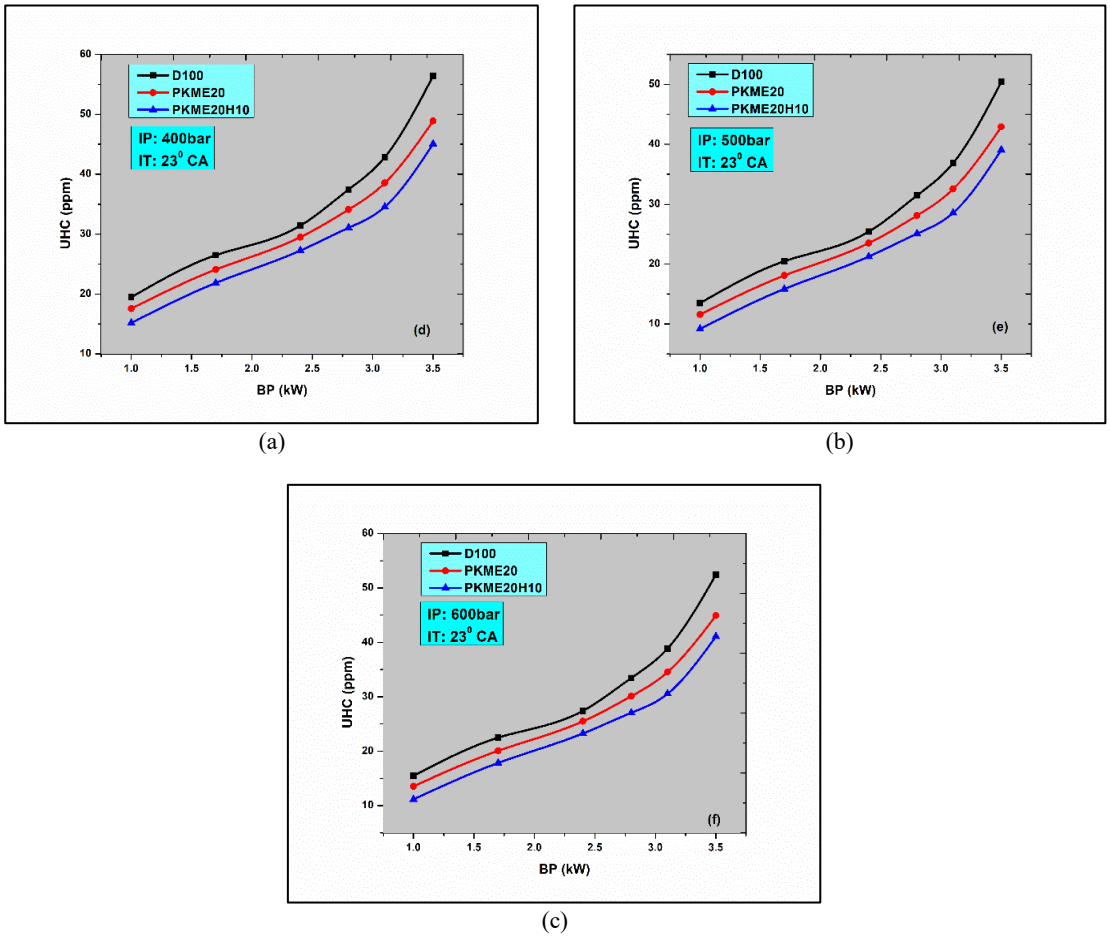

Fig. 9. Variation of unburnt hydrocarbon emissions (UHC): (a) 400 bar, (b) 500 bar, and (c) 600 bar.

Carbon monoxide emission

A scarcity of oxygen or a reduction in temperature inside the cylinder helps prevent carbon monoxide from converting into carbon dioxide after getting oxidized. The advancement in the timing of injection leads to enhancements of CO emissions as seen from the results. Since most fuel is used in pre-mixture combustion, advanced injection timing lowers bulk cylinder temperatures and CO_2 oxidation (Gültekin et al., 2024; Panda et al., 2025). At 600 bar, injection pressure increases CO emissions, whereas at 500 bar, finer atomization improves combustion. Advanced injection timing for PKME20, diesel, and PKME20H10 increases CO emissions at 600 pressure. Improper air-fuel mixture compromises combustion efficiency, primarily affecting CO emissions (Seelam et al., 2022; Vadlamudi et al., 2023a, 2023b). Raising injection pressure (Fig 10) to 500 bar from 400 bar enhances combustion, reducing CO levels. The PKME20H10 blend achieves complete combustion, lowering CO emissions by 16% at 23° CA bTDC and 500 bar injection pressure, potentially resulting in reduced CO_2 emissions due to higher oxygen content. Hydrogen inclusion in the blend further reduces both CO and CO_2 emissions, as hydrogen's diffusivity and reduced carbon intake enhance combustion efficiency.

https://doi.org/10.24191/jmeche.v23i1.8763

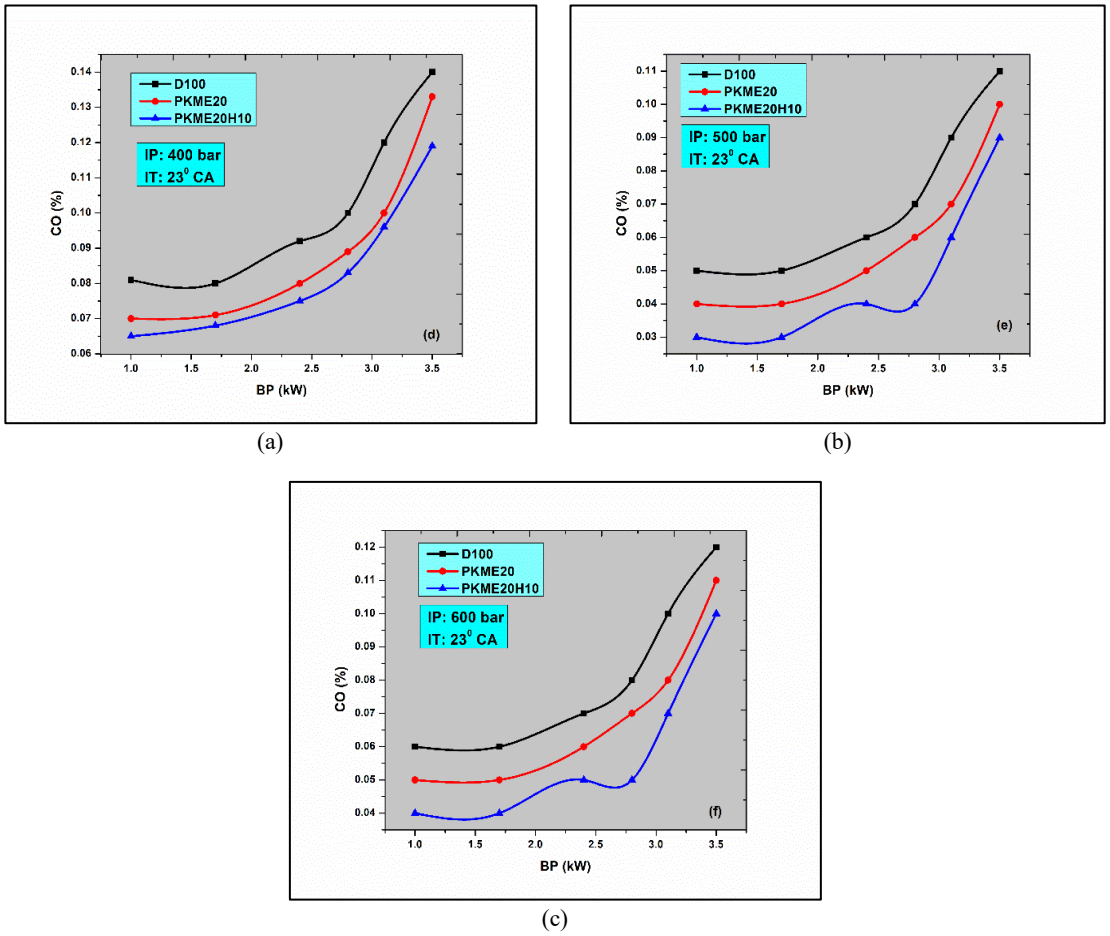

Fig. 10. Variation of CO: (a) 400 bar, (b) 500 bar, and (c) 600 bar.

The pronounced decrease in UHC (≈45%) and CO (≈16%) emissions for PKME20H10 relative to diesel agrees with the experimental outcomes of Loganathan et al. (2020) and Vadlamudi et al. (2025), who documented significant reductions in incomplete combustion species with biodiesel–hydrogen mixtures. This correspondence validates that hydrogen addition promotes complete oxidation by expanding the flammability range and enhancing air–fuel mixing.

Smoke opacity

With an increase in injection pressure, the smoke opacity levels were observed to be decreased (Fig 11). As per the observed pattern, with the increase in fuel injection timing, smoke opacity levels decreased. Lesser fuel rich zones were observed due to the uniformity in air fuel mixture caused by better atomization of fuel. Thus, the formation of soot also decreased significantly. Moreover, the availability of spare time during the mixing of air and fuel also causes a reduction in soot formation. At 23° CA bTDC and 500 bar, the levels of smoke were 28.7% lesser than diesel at higher loads. The smoke opacity reduces significantly at higher injection pressure due to uniformity in the air-fuel mixture, and is caused by the introduction of hydrogen which has a higher diffusivity. The smoke opacity rises above the pressure of 600 bar, subject to the delay in injection at higher injection pressure.

https://doi.org/10.24191/jmeche.v23i1.8763

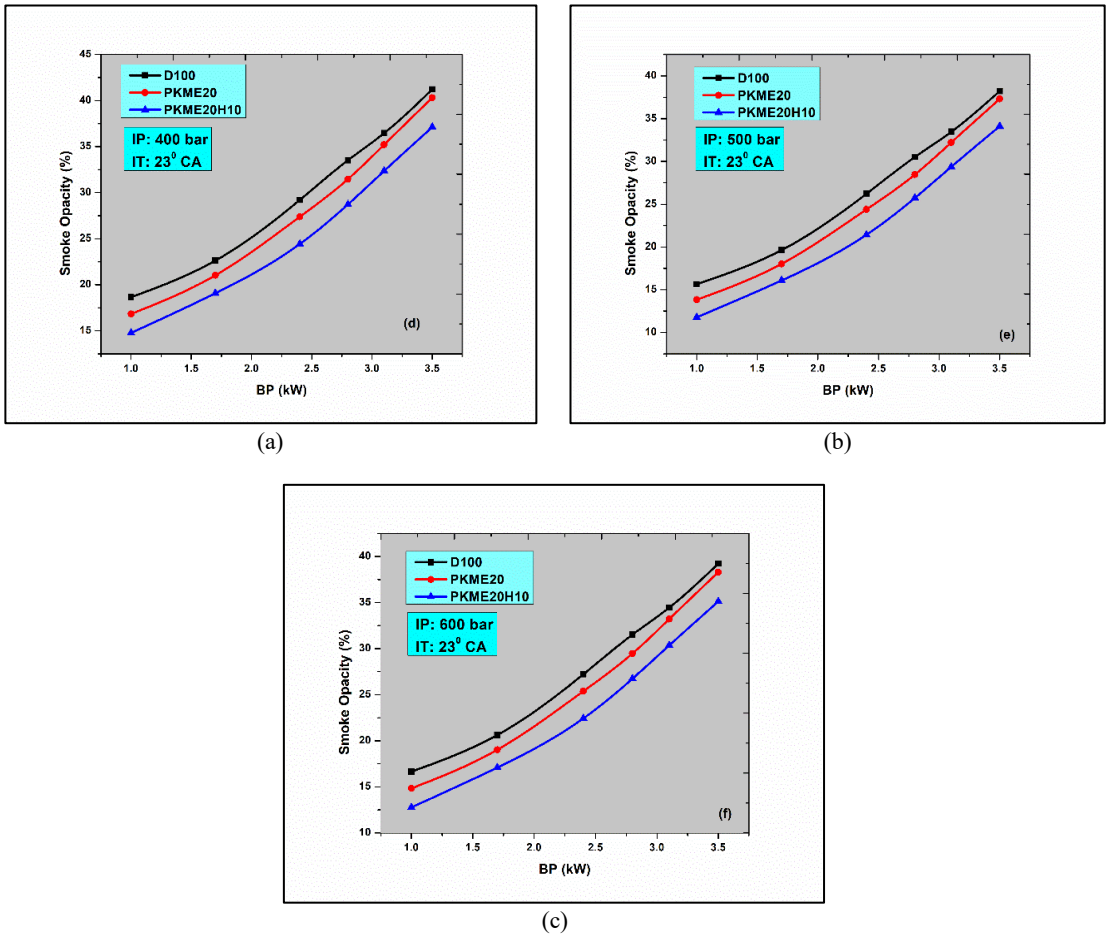

Fig. 11. Variation of smoke: (a) 400 bar, (b) 500 bar, and (c) 600 bar.

Oxides of nitrogen

An improved combustion is achieved due to a negligible rise in NOx emissions at advanced injection timings and a better mixture of the air and fuel during the combustion (Fig 12). This is mainly due to the elevated temperature of the combustion cylinder, that raises the rate of Nox emission produced. High injection pressure causes this combustion type with high NOx and cylinder temperature. At 23° CA bTDC and 500 bar, PKME20 and PKME20H10 have greater NOx levels (7.25% and 10.3%, respectively) than pure diesel. NOx emissions increase due to a rise in temperature inside the cylinder caused by hydrogen's higher calorific value in addition to a change in injection pressure from 400 to 500 bar. The pilot injection pressure rises to a maximum when the internal temperature of the cylinder is higher, and the combustion takes place much quicker. The decline in temperature is more in the case of 600 bar injection pressure as compared to 500 bar due to partial combustion (Akcay et al., 2021; Vadlamudi et al., 2025).

https://doi.org/10.24191/jmeche.v23i1.8763

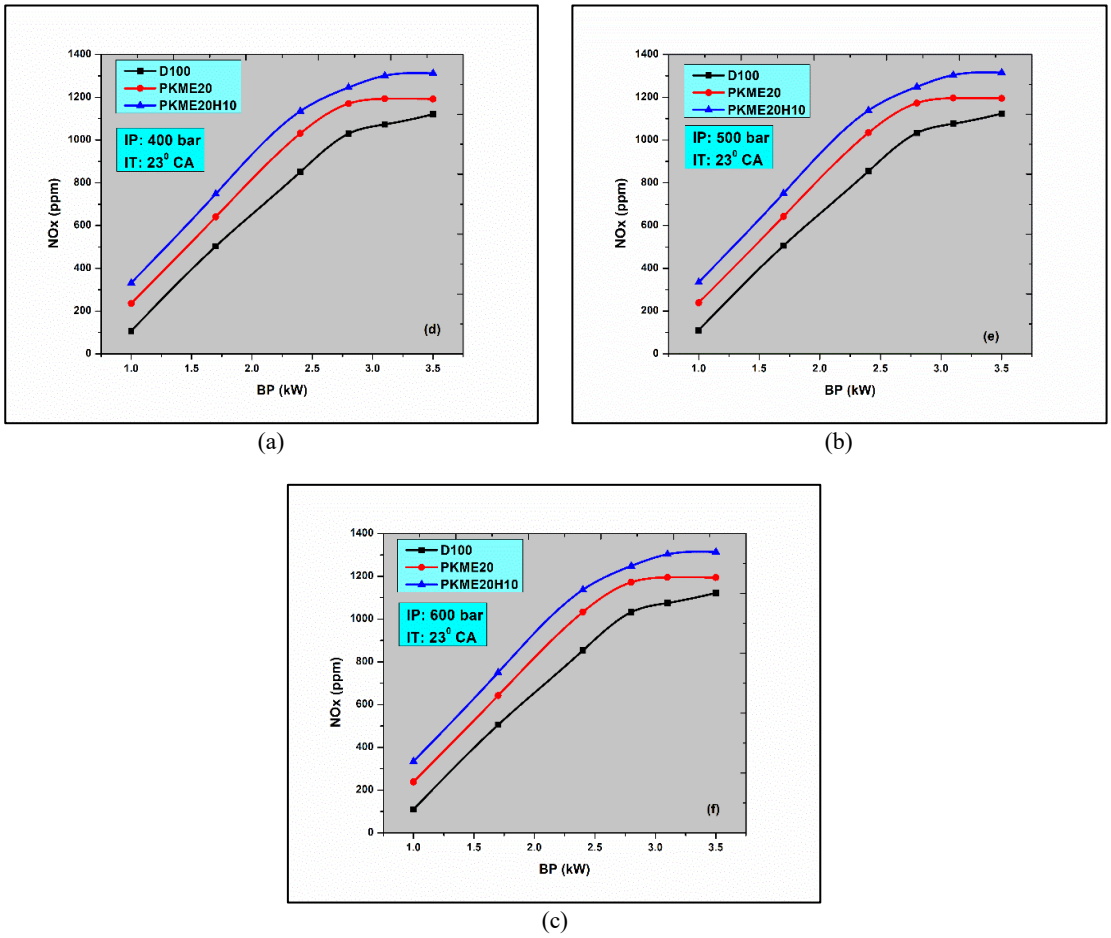

Fig. 12. Variation of NOX: (a) 400 bar, (b) 500 bar, and (c) 600 bar.

Although NOx emissions increased by about 10% for PKME20H10 compared to D100, this behavior is consistent with Arslan & Kahraman (2022) and Mohite et al. (2024b), who also reported a similar NOx rise due to elevated combustion temperatures in hydrogen-assisted biodiesel operation. Nonetheless, the concurrent 28.7% reduction in smoke opacity underscores the clean combustion advantage of the proposed blend. The balance achieved between NOx increase and reductions in CO, HC, and smoke confirms the environmental suitability of hydrogen–biodiesel fuels.

Artificial neural network strategy

Artificial neural networks (ANNs) learn from data via a structured process. This training involves building the network and applying both feed-forward and back-propagation techniques. In feed-forward, neuron outputs are determined based on input strengths (Dahake et al., 2024; Liao et al., 2023). In the back propagation method to improve the model performance, the network weights are updated with respect to minimization of mean squared error (MSE). This process of improving of the network performance is continued for several iterations through adjusting the weights during the training program. The MATLAB platform was used in this case of study to utilize the ANN solver for modelling. In this study, the total dataset is divided randomly in three parts by 70%, 15% and 15% respectively, for training, validation, and testing of the trained network. Selecting the right training rule is crucial for adjusting network weights,

https://doi.org/10.24191/jmeche.v23i1.8763

aiming to reduce the error between actual and predicted outputs. This research adopts the Levenberg-Marquardt backpropagation for its fast convergence. It utilizes the log-sigmoid function for activation due to its smooth differentiability. To scale inputs and outputs, a logistic sigmoid function is employed. The study minimizes error using the mean squared error (MSE) loss function (Pitchaiah et al., 2023; Wang et al., 2023).

In this study, statistical models for various output factors in order to simulate engine system reaction in terms of performance, emissions, and combustion characteristics were developed. The engine response or output parameters that were taken into consideration for the development of the ANN model were BSFC, BTE, NOx, smoke, UHC, and CO, while the control factors considered for this study were load, injection timing, injection pressure, diesel, biodiesel, and hydrogen share. The models' forecasting accuracy was evaluated using correlation, MAPE (Mean Absolute Percentage Error) for absolute error, and RRSE (Root Relative Squared Error) for relative error, as described by the equations. The outcomes of the ANN analyses across various output parameters are depicted in Figs 13(a-f).

$$MAPE = \frac{1}{m}\sum_{n=1}^{m}\left(\left|\frac{e_n - Ap_n}{e_n}\right|\right) \times 100 \tag{1}$$

$$RRSE = \sqrt{\frac{\sum_{n=1}^{m}(Ap_n - e_n)^2}{\sum_{n=1}^{m}(e_n - e_{av})^2}} \tag{2}$$

where:

m	:	number of experimentations
e_n	:	experimental values
Ap_n	:	ANN predicted values of output and
Ap_{av}	:	average of experimental values of output

ANN performance model evaluation

The ANN-based BSFC (Fig 13(a)) model showed high precision with MAPE and RRSE errors at 0.13 and 0.1, respectively. Additionally, the ANN model for BTE (Fig 13(b)) displayed a strong correlation (R = 0.998), highlighting its accurate predictive performance. A closer examination of BTE's model indicated significantly reduced MAPE and RRSE values, confirming the model's exceptional forecasting capability for engine performance parameters.

ANN emissions model evaluation

The ANN model's NOx predictions, with low MAPE and RRSE values in Fig 13(c), highlight its precision. Similarly, smoke predictions by the model showed a high R value in Fig 13(d), underscoring its accuracy. The model's reliability was confirmed by MAPE and RRSE values of 0.22 and 0.25, respectively, in Fig 14. The UHC model, with a high R value shown in Fig 13(e), and low error rates in Fig 14, demonstrated its accurate emission forecasting. The CO emission model, revealing a 0.995 R value in Fig 13(f) and low errors in Fig 14, further validated the ANN model's predictive strength across various emissions.

https://doi.org/10.24191/jmeche.v23i1.8763

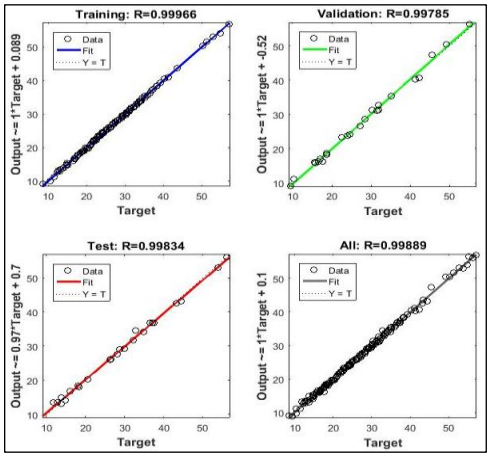

(a)

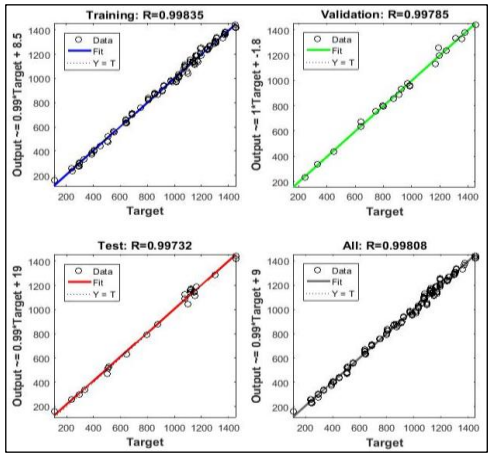

(b)

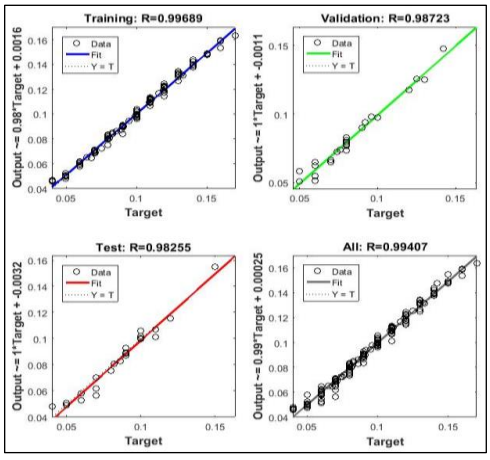

(c)

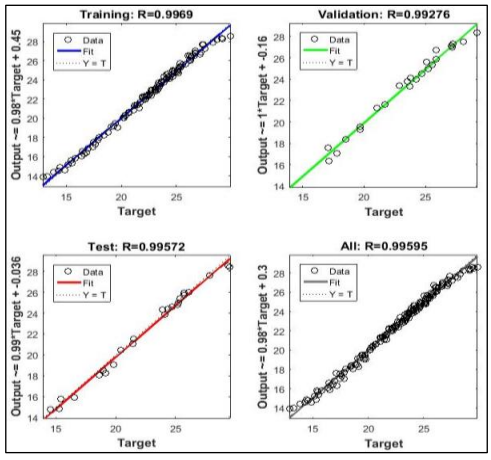

(d)

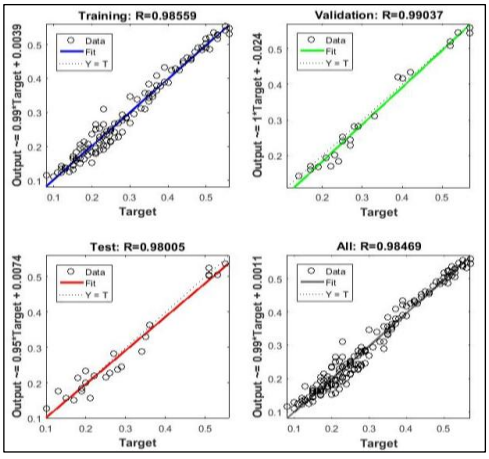

(e)

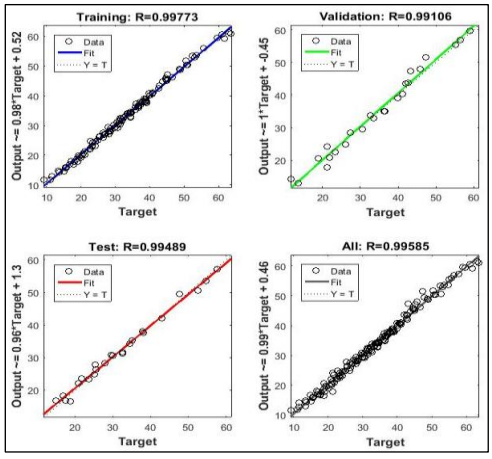

(f)

Fig. 13. Predicted vs targeted value: (a) BSFC, (b) BTE, (c) NOx, (d) smoke, (e) UHC and (f) CO.

https://doi.org/10.24191/jmeche.v23i1.8763

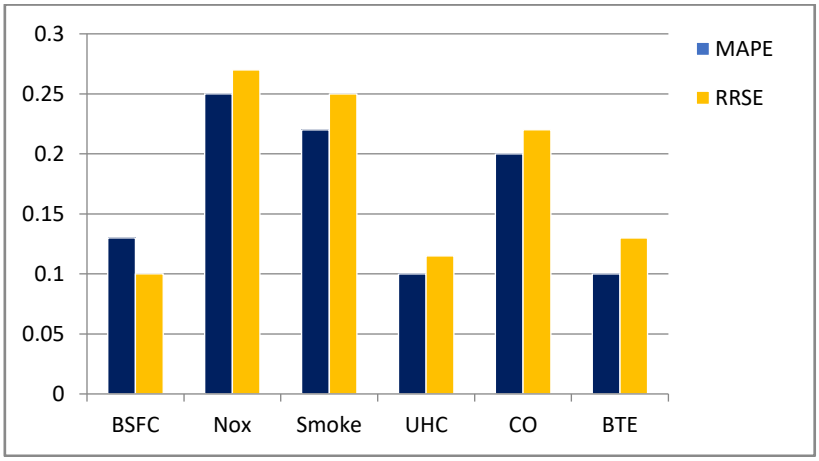

Fig. 14. MAPE and RRSE error values of developed ANN metamodels.

Selection of the best fuel strategy

The fuel strategy for D100, PKME20, and PKME20H10 for 6 different BP levels of 1 kW to 3.5 kW at 400, 500, and 600 bar injection pressure, 21° CA bTDc, 22° CA bTDC, 23° CA bTDC was studied. A total of 162 experiments were performed in this study. These datasets were then utilized to develop metamodels for each output factors using Artificial neural network. A total of 162 distinct experimental test combinations were derived from the matrix of three fuels (D100, PKME20, PKME20H10), three injection pressures (400, 500, and 600 bar), three injection timings (21°, 23°, and 25° CA bTDC), and six load conditions (1.0 kW – 3.5 kW). Each test point represents an independent operating condition, and the steady-state results were averaged from three repeated runs to ensure reliability. After that, the NSGA II algorithm was used to explore the sets of input factors that have the potential to provide optimal desired responses. The maximization of BTE and minimization of BSFC, as well as emission profiles of UHC, smoke, and NOx have been encapsulated in terms of mathematical problems in Equations 3 and 4, respectively.

$$Maximize \begin{bmatrix} BTE \\ BSFC \end{bmatrix} = f_{ANN}(BTE) \tag{3}$$

$$Minimize \begin{bmatrix} UHC \\ SMOKE \\ NOx \end{bmatrix} = f_{ANN}(BSFC, UHC, SMOKE, NOx) \tag{4}$$

The parametric configuration of NSGA II used in this study is demonstrated in Table 5. The NSGA II performed a computational study with 50 populations and 100 generations. However, all the solutions as shown in Table 6 represent optimal solutions from which selecting one optimal solution is a difficult task (Wang et al., 2023). For this reason, TOPSIS has been applied to these solutions to find the best compromised solution (Zeng et al., 2023). Table 5 presents the Pareto-optimal results obtained from the ANN–NSGA-II optimization process. Each dataset corresponds to a unique combination of injection timing, injection pressure, and load conditions for the three tested fuels. The optimal ranked solution (Rank 1) corresponds to the PKME20H10 fuel at 3.5 kW load, 512 bar injection pressure, and 25° CA bTDC injection timing, representing the most balanced trade-off between performance and emissions.

https://doi.org/10.24191/jmeche.v23i1.8763

Table 5. NSGA II parametric configuration

Parameter	Values
No of population	50
No of generations	100
Parent selection strategy	Binary tournament selection
Mutation	0.02
Cross over	0.7

Table 6. Decision table for TOPSIS based on performance index (rank)

Gen. No	BTE	BSFC	UHC	SMOKE	NOX	Rank
1	25.39	0.26	27.91	46.44	1001.84	40
2	22.30	0.34	21.87	30.68	948.01	16
3	27.67	0.24	19.60	46.46	1185.39	32
4	25.96	0.33	21.00	49.09	1035.39	24
5	20.95	0.15	28.64	47.95	906.27	34
6	21.66	0.36	22.93	52.56	942.26	23
7	26.15	0.25	26.90	46.68	1009.61	42
8	20.67	0.34	26.30	37.94	1023.65	46
9	20.93	0.35	25.74	48.25	1001.58	37
10	21.26	0.36	27.41	41.89	956.12	29
11	30.12	0.12	15.55	24.42	756.80	1
12	20.72	0.36	24.11	47.38	931.26	18
13	26.83	0.35	29.19	37.40	990.71	47
14	26.26	0.25	22.03	31.41	899.70	3
15	21.14	0.14	25.87	48.21	892.95	28
16	23.56	0.3	28.29	46.70	988.11	44
17	21.54	0.35	21.82	37.01	879.95	2
18	26.85	0.15	26.58	48.16	984.36	39
19	24.09	0.35	23.24	36.13	995.94	20
20	20.79	0.34	21.44	47.84	946.50	8
21	21.45	0.17	25.84	48.40	994.14	35
22	20.82	0.32	21.95	51.39	962.23	22
23	27.80	0.22	23.05	37.56	1005.32	30
24	21.07	0.25	23.20	46.02	969.58	17
25	20.47	0.32	20.99	50.68	905.70	10
26	20.82	0.23	22.73	47.31	985.13	21
27	20.86	0.34	24.80	48.46	920.86	27
28	20.86	0.22	28.96	25.99	988.83	49
29	23.52	0.37	18.53	48.13	976.32	12
30	24.89	0.34	22.44	51.65	973.28	31
31	30.09	0.15	26.91	46.86	1003.23	41
32	21.56	0.21	22.49	49.11	910.35	9
33	21.48	0.13	29.04	50.81	990.00	50
34	25.32	0.15	23.39	49.93	856.92	7

https://doi.org/10.24191/jmeche.v23i1.8763

35	20.78	0.34	28.58	50.65	962.64	48
36	20.88	0.33	21.67	48.02	946.27	11
37	23.92	0.36	22.83	51.37	789.58	4
38	20.56	0.35	23.39	49.67	924.23	19
39	26.92	0.16	24.93	48.00	933.41	26
40	21.19	0.25	22.52	46.96	923.61	6
41	20.93	0.18	26.15	47.51	982.36	36
42	22.00	0.34	26.60	41.99	1020.59	45
43	20.82	0.35	27.20	47.18	1003.04	43
44	22.10	0.23	21.06	46.94	1080.15	25
45	21.01	0.25	27.49	47.32	968.81	38
46	20.79	0.35	23.02	46.88	955.24	15
47	26.08	0.35	25.52	49.96	814.52	14
48	22.18	0.17	22.85	50.74	907.71	13
49	21.06	0.22	26.21	48.91	944.30	33
50	21.38	0.21	27.34	36.70	887.50	5

The input conditions for Table 6 are derived from a multi-variable experimental matrix combining three fuel types (D100, PKME20, PKME20H10), three injection pressures (400, 500, and 600 bar), and three injection timings (21°, 23°, and 25° CA bTDC), tested across six brake power levels (1 kW – 3.5 kW). These combinations yielded 162 experiments to develop ANN-based metamodels for engine outputs, which were then optimized using NSGA-II. The TOPSIS method was applied to identify the best compromise solution from these Pareto-optimal outputs, focusing on maximizing BTE and minimizing BSFC, NOx, UHC, and smoke.

The optimal solution identified in Table 5, ranked first using the TOPSIS method, corresponds to a brake thermal efficiency (BTE) of 30.12%, brake-specific fuel consumption (BSFC) of 0.12 kg/kWh, unburnt hydrocarbon (UHC) emissions of 15.55 ppm, smoke opacity of 24.42%, and nitrogen oxide (NOx) emissions of 756 ppm. These values were achieved under the input conditions of 3.5 kW brake power (BP), 25° crank angle before top dead center (CA bTDC) injection timing, and 512 bar injection pressure using the PKME20H10 fuel blend (20% palm kernel biodiesel, 70% diesel, and 10 lpm hydrogen). The selection of 3.5 kW as the optimal BP is significant as it represents the highest load tested, where engine parameters are most strained, making efficiency and emission improvements most impactful. The advanced injection timing (25° CA bTDC) allows for better air-fuel mixing, promoting complete combustion, while the elevated injection pressure (512 bar) ensures fine fuel atomization, enhancing the overall combustion process. Hydrogen's high diffusivity and calorific value further improve combustion quality, contributing to lower emissions and better efficiency. This combination of inputs yields a balanced trade-off between performance enhancement and emission reduction, validating the hybrid optimization strategy (ANN + NSGA-II + TOPSIS) employed in the study.

Table 7 presents a comparative validation of the optimal solution derived from the computational study against actual experimental results. The optimal parameters, 3.5 kW brake power, 25° CA bTDC injection timing, and 512 bar injection pressure using the PKME20H10 fuel blend, were experimentally tested to confirm the accuracy of the predicted outputs. The table lists six key engine response parameters: BTE, BSFC, UHC, smoke, NOx, and CO. For each parameter, the computational and experimental values are compared, and the percentage error is calculated. The deviations for all parameters lie below 5%, indicating strong agreement between the ANN-NSGA-II-TOPSIS model and real-world engine behavior. For example, BTE showed a negligible deviation of 0.07%, while BSFC had a slight variation of -2.5%.

https://doi.org/10.24191/jmeche.v23i1.8763

Similarly, emissions such as UHC, smoke, and NOx deviated by only 2.9%, 3.56%, and 3.67% respectively, validating the robustness of the optimization model. Although the CO value wasn't computed in the ANN model, its experimental value (0.09%) supports the overall emission reduction trend. This table not only confirms the predictive accuracy of the artificial intelligence-driven optimization approach but also strengthens confidence in applying such hybrid strategies for real-time engine calibration, enabling a reliable and efficient shift toward greener fuel technologies.

Table 7. Deviation of computational data from actual experimental value

Sl No	Responses	Computational value (C)	Experimental value (E)	Error (%) = (C-E) × 100/C
1	BTE	30.12	30.10	0.07
2	BSFC	0.12	0.11	-2.5
3	UHC	15.55	15.11	2.9
4	Smoke	24.42	23.55	3.56
5	NOx	756.80	729	3.67
6	CO	-	0.09	-

In comparison with conventional optimization techniques, the proposed hybrid ANN–NSGA-II–TOPSIS model demonstrates superior adaptability and prediction accuracy for nonlinear engine behavior. While RSM has been widely applied for parametric optimization, its polynomial-based models often underperform when handling high-dimensional or strongly coupled variables such as injection timing, pressure, and fuel blend ratio (Wang et al., 2023). Classical GA and PSO methods, though capable of exploring global optima, rely on randomly generated populations and do not inherently incorporate learned system behavior. In contrast, ANN captures the underlying nonlinear mapping between input and output responses, providing accurate surrogate models that guide the NSGA-II search process. The inclusion of TOPSIS further refines multi-objective decision-making by identifying the most balanced solution among the Pareto front. This integrated strategy results in improved predictive accuracy ($R > 0.99$) and lower MAPE (< 3%) compared with the single optimization approaches reported in earlier hydrogen–biodiesel optimization studies (Mohite et al., 2024b; Kanth et al., 2020; Akcay et al., 2021).

CONCLUSIONS

This study evaluates injection timing and pressure effects on performance and emissions of hydrogen-enriched PKME20 in engines via ANN–NSGA-II–TOPSIS optimization. The research aimed to identify an optimal operating strategy that maximizes thermal efficiency while minimizing exhaust emissions. The experimental findings, reinforced through computational optimization, revealed that the optimal combination of 3.5 kW load, an injection timing of 25° CA bTDC, and an injection pressure of 512 bar achieved a BTE of 30.1% and a BSFC of 0.123 kg/kWh, along with notable emission reductions, including a 10% decrease in CO, a 45% reduction in unburnt hydrocarbons, and a 17% reduction in smoke opacity compared with diesel baseline operation

The study's novelty lies in coupling a data-driven ANN model with multi-objective optimization to derive precise control parameters for hydrogen-biodiesel combustion. This approach effectively bridges experimental and computational domains, offering a replicable framework for clean-fuel optimization in advanced diesel systems. While the results confirm hydrogen's potential to enhance combustion and efficiency, a moderate increase in NOx emissions remains a limitation that warrants further mitigation through EGR or after-treatment integration. Future research may extend this hybrid methodology to multi-cylinder engines, transient operating conditions, and alternative gaseous fuels such as HHO or ammonia blends to validate scalability.

https://doi.org/10.24191/jmeche.v23i1.8763

In summary, this study establishes PKME20H10 as a promising green alternative to diesel and demonstrates the capability of hybrid AI-based optimization in achieving a sustainable balance between engine performance, fuel economy, and emission control.

ACKNOWLEDGEMENTS/ FUNDING

The authors thank Anurag University, Hyderabad, India and Apex Lab, Pune, India for providing the facilities and kind support.

CONFLICT OF INTEREST STATEMENT

The authors agree that this research was conducted in the absence of any self-benefits, commercial or financial conflicts and declare the absence of conflicting interests with the funders.

AUTHORS' CONTRIBUTIONS

P. Ajay Goud: conceptualization, experimental design, data curation, methodology development, investigation, writing original draft preparation. Mohammad Sikindar Baba: supervision, validation, formal analysis, interpretation of results, writing review & editing, project administration.

REFERENCE

Akcay, M., Yilmaz, I. T., & Feyzioglu, A. (2020). Effect of hydrogen addition on performance and emission characteristics of a common-rail CI engine fueled with diesel/waste cooking oil biodiesel blends. Energy, 212, 118538. https://doi.org/10.1016/j.energy.2020.118538

Akcay, M., Yilmaz, I. T., & Feyzioglu, A. (2021). The influence of hydrogen addition on the combustion characteristics of a common-rail CI engine fueled with waste cooking oil biodiesel/diesel blends. Fuel Processing Technology, 223, 106999. https://doi.org/10.1016/j.fuproc.2021.106999

Anand, T., & Debbarma, S. (2024). Experimental analysis of hydrogen enrichment in waste plastic oil blends for dual-fuel common rail direct injection diesel engines. Journal of Energy Resources Technology, 146(1), 012302. https://doi.org/10.1115/1.4063665

Anderson, A., Karthikeyan, L., Sahoo, D. K., Mallika, M., & Prakash, S. (2023). Numerical analysis of spray characteristics with methane and nanoparticles under various injection velocities. Journal of Energy Resources Technology, 145(8), 084501. https://doi.org/10.1115/1.4062379

Arslan, E., & Kahraman, N. (2022). The effects of hydrogen enriched natural gas under different engine loads in a diesel engine. International Journal of Hydrogen Energy, 47(24), 12410-12420. https://doi.org/10.1016/j.ijhydene.2021.09.016

Bhowmik, C., Deb, M., Tarafdar, A., Panda, J. K., Bhiradi, I., Thirugnanasambandam, A., & Gugulothu, S. K. (2025). AI-driven performance and emission forecasting in diesel–hydrogen dual-fuel engines: a machine learning approach. Journal of Thermal Analysis and Calorimetry, 150(25), 20815-20846. https://doi.org/10.1007/s10973-025-14998-9

https://doi.org/10.24191/jmeche.v23i1.8763

Dahake, M. R., Gajjal, P. S., Barhatte, A. S., & Malkhede, D. N. (2024). Experimental exploration of hydrogen fuelled dual fuelled CRDI equipped diesel engine coupled with exhaust gas recirculation using ANN approach. International Journal of Ambient Energy, 45(1), 2280732. https://doi.org/10.1080/01430750.2023.2280732

Debbarma, S., Misra, R. D., & Das, B. (2020). Performance of graphene-added palm biodiesel in a diesel engine. Clean Technologies and Environmental Policy, 22(2), 523-534. https://doi.org/10.1007/s10098-019-01800-2

Farooq, M. S., Baig, A., Wei, Y., & Liu, H. (2024). Comprehensive review on technical developments of methanol-fuel-based spark ignition engines to improve the performance, combustion, and emissions. Journal of Energy Resources Technology, 146(7), 070801. https://doi.org/10.1115/1.4065249

Gültekin, N., Gülcan, H. E., & Ciniviz, M. (2024). Investigation of the effects of hydrogen energy ratio and valve lift amount on performance and emissions in a hydrogen-diesel dual-fuel compression ignition engine. International Journal of Hydrogen Energy, 49(B), 352-366. https://doi.org/10.1016/j.ijhydene.2023.07.294

Holman, J. P., & Gajda, W. J. (1978). Experimental methods for engineers. McGraw-Hill.

Isler-Kaya, A., & Karaosmanoglu, F. (2023). Fatty acid ethyl esters obtained from safflower oil: a fully renewable biofuel. Journal of Energy Resources Technology, 145(10), 101302. https://doi.org/10.1115/1.4062870

Jabbr, A. I., & Koylu, U. O. (2019). Influence of operating parameters on performance and emissions for a compression-ignition engine fueled by hydrogen/diesel mixtures. International Journal of Hydrogen Energy, 44(26), 13964-13973. https://doi.org/10.1016/j.ijhydene.2019.03.201

Jamrozik, A., Grab-Rogaliński, K., & Tutak, W. (2020). Hydrogen effects on combustion stability, performance and emission of diesel engine. International Journal of Hydrogen Energy, 45(38), 19936-19947. https://doi.org/10.1016/j.ijhydene.2020.05.049

Jia, G., Gao, S., Shu, X., Ren, B., Zhang, B., Ma, G., Zhang, J., Liu, H., & Li, D. (2024). Multi-objective optimization of emission parameters of a diesel engine using oxygenated fuel and pilot injection strategy based on RSM-NSGA III. Energy, 293, 130661. https://doi.org/10.1016/j.energy.2024.130661

Kanth, S., Debbarma, S., & Das, B. (2020). Effect of hydrogen enrichment in the intake air of diesel engine fuelled with honge biodiesel blend and diesel. International Journal of Hydrogen Energy, 45(56), 32521-32533. https://doi.org/10.1016/j.ijhydene.2020.08.152

Kumar, V., & Choudhary, A. K. (2023). A hybrid response surface methodology and multi-criteria decision making model to investigate the performance and emission characteristics of a diesel engine fueled with phenolic antioxidant additive and biodiesel blends. Journal of Energy Resources Technology, 145(9), 092302. https://doi.org/10.1115/1.4056939

Liao, W. R., Shi, J. H., & Li, G. X. (2023). CRDI engine emission prediction models with injection parameters based on ANN and SVM to improve the SOOT-NOx trade-off. Journal of Applied Fluid Mechanics, 16(10), 2041-2053. https://doi.org/10.47176/jafm.16.10.1801

Loganathan, M., Thanigaivelan, V., Madhavan, V. M., Anbarasu, A., & Velmurugan, A. (2020). The synergetic effect between hydrogen addition and EGR on cashew nut shell liquid biofuel-diesel operated engine. Fuel, 266, 117004. https://doi.org/10.1016/j.fuel.2019.117004

Mohite, A., Bora, B. J., Sharma, P., Medhi, B. J., Barik, D., Balasubramanian, D., Nguyen, V. G., Femilda Josephin, J. S., Le, H. C., Kamalakannan, J., Varuvel, E. G., & Cao, D. N. (2024a). Maximizing

https://doi.org/10.24191/jmeche.v23i1.8763

efficiency and environmental benefits of an algae biodiesel-hydrogen dual fuel engine through operational parameter optimization using response surface methodology. International Journal of Hydrogen Energy, 52(D), 1395-1407. https://doi.org/10.1016/j.ijhydene.2023.10.134

Mohite, A., Bora, B. J., Ağbulut, Ü., Sharma, P., Medhi, B. J., & Barik, D. (2024b). Optimization of the pilot fuel injection and engine load for an algae biodiesel-hydrogen run dual fuel diesel engine using response surface methodology. Fuel, 357(B), 129841. https://doi.org/10.1016/j.fuel.2023.129841

Nibin, M., Varuvel, E. G., Femilda Josephin, J. S., & Vikneswaran, M. (2024). Evaluation of wheat germ oil biofuel in diesel engine with hydrogen, bioethanol dual fuel and fuel ionization strategies. International Journal of Hydrogen Energy, 59, 889-902. https://doi.org/10.1016/j.ijhydene.2024.02.067

Nithya, S., Jeyaseelan, G. A. C., Ali Alharbi, S., Alfarraj, S., & Jhanani, G. K. (2023). Prediction of waste chicken fat biodiesel blends as the potential substitute for the diesel engine with oxygenated additives. Journal of Energy Resources Technology, 145(9), 091301. https://doi.org/10.1115/1.4057031

Panda, J. K., Peng, J., Deb, P., Rajesh, K., Vadlamudi, S., Dewangan, N. K., Pachauri, N., & Kumari, S. (2025). A novel paradigm CNG dual-fuel strategy to reduce engine emission of a CRDI engine: a green fuel and multi-objective optimization approach. Journal of Mechanical Engineering, 22(1), 176-190. https://doi.org/10.24191/jmeche.v22i1.4562

Pitchaiah, S., Juchelková, D., Sathyamurthy, R., & Atabani, A. E. (2023). Prediction and performance optimisation of a DI CI engine fuelled diesel–Bael biodiesel blends with DMC additive using RSM and ANN: energy and exergy analysis. Energy Conversion and Management, 292, 117386. https://doi.org/10.1016/j.enconman.2023.117386

Prabhu, L., Shenbagaraman, S., Anbarasu, A., Muniappan, A., Suthan, R., & Veza, I. (2023a). Prediction of the engine performance and emission characteristics of Glycine max biodiesel blends with nanoadditives and hydrogen. Journal of Energy Resources Technology, 145(11), 112701. https://doi.org/10.1115/1.4062380

Prabhu, L., Dhanalakshmi, K., Alahmadi, T. A., Alharbi, S. A., Sołowski, G., & Veeman, D. (2023b). How do microalgae biodiesel blends affect the acoustic and vibration characteristics of the direct injection diesel engine: an experimental examination. Journal of Energy Resources Technology, 145(11), 112101. https://doi.org/10.1115/1.4056797

Praveenkumar, T. R., Rath, B., Devanesan, S., Alsahi, M. S., Jhanani, G. K., Gemede, H. F., Solowski, G., & Daniel, F. (2023). Performance and emission characteristics for karanja biodiesel blends assisted with green hydrogen fuel and nanoparticles. Journal of Energy Resources Technology, 145(11), 112702. https://doi.org/10.1115/1.4062526

Ramachander, J., Gugulothu, S. K., Sastry, G. R. K., Panda, J. K., & Surya, M. S. (2021). Performance and emission predictions of a CRDI engine powered with diesel fuel: a combined study of injection parameters variation and Box-Behnken response surface methodology-based optimization. Fuel, 290, 120069. https://doi.org/10.1016/j.fuel.2020.120069

Runyon, J., James, S., Kadam, T., Ofir, B., & Graham, D. (2024). Performance, emissions, and decarbonization of an industrial gas turbine operated with hydrotreated vegetable oil. Journal of Engineering for Gas Turbines and Power, 146(6), 061020. https://doi.org/10.1115/1.4063787

Santhosh, K., & Kumar, G. N. (2021). Effect of hydrogen and 1-Hexanol on combustion, performance and emission characteristics of CRDI CI engine. Fuel, 285, 119100. https://doi.org/10.1016/j.fuel.2020.119100

https://doi.org/10.24191/jmeche.v23i1.8763

Seelam, N., Gugulothu, S. K., Reddy, R. V., Bhasker, B., & Panda, J. K. (2022). Exploration of engine characteristics in a CRDI diesel engine enriched with hydrogen in dual fuel mode using toroidal combustion chamber. International Journal of Hydrogen Energy, 47(26), 13157-13167. https://doi.org/10.1016/j.ijhydene.2022.02.056

Shen, T., Wu, Y., Alahmadi, T. A., Alharbi, S. A., Maroušek, J., Xia, C., & Praveenkumar, T. R. (2023). Assessment of combustion and acoustic characteristics of Scenedesmus dimorphus blended with hydrogen fuel on internal combustion engine. Journal of Energy Resources Technology, 145(5), 052302. https://doi.org/10.1115/1.4056446

Sun, P., Cheng, X., Yang, S., Ruan, E., Zhao, H., Liu, Y., & Zhao, C. (2024). Artificial neural network models for forecasting the combustion and emission characteristics of ethanol/gasoline DFSI engines with combined injection strategy. Case Studies in Thermal Engineering, 54, 104007. https://doi.org/10.1016/j.csite.2024.104007

Tayari, S., & Abedi, R. (2019). Effect of Chlorella vulgaris methyl ester enriched with hydrogen on performance and emission characteristics of CI engine. Fuel, 256, 115906. https://doi.org/10.1016/j.fuel.2019.115906

Vadlamudi, S., Gugulothu, S. K., Panda, J. K., & Ağbulut, Ü. (2025). Machine learning based hydrogen fuel approach: a detailed experimental study on CRDI engine performance, combustion, and environmental characteristics. Energy, 336, 138345. https://doi.org/10.1016/j.energy.2025.138345

Vadlamudi, S., Gugulothu, S. K., Panda, J. K., Deepanraj, B., & Kumar, P. R. V. (2023a). Paradigm analysis of performance and exhaust emissions in CRDI engine powered with hydrogen and hydrogen/CNG fuels: a green fuel approach under different injection strategies. International Journal of Hydrogen Energy, 48(96), 38059-38076. https://doi.org/10.1016/j.ijhydene.2022.08.277

Vadlamudi, S., Gugulothu, S. K., Panda, J. K., Deepanraj, B., & Kumar, P. R. V. (2023b). Trade-off study on environmental-economical aspects of a CRDI engine using hydrogen as dual fuel mode powered with different low viscous alcohol additives. International Journal of Hydrogen Energy, 48(96), 38044-38058. https://doi.org/10.1016/j.ijhydene.2022.07.234

Wang, Y., Wang, G., Yao, G., Shen, Q., Yu, X., & He, S. (2023). Combining GA-SVM and NSGA-III multi-objective optimization to reduce the emission and fuel consumption of high-pressure common-rail diesel engine. Energy, 278(A), 127965. https://doi.org/10.1016/j.energy.2023.127965

Zeng, H., Jiang, K., Wu, Z., & Liu, X. (2023). Performance research and optimization of marine dual-fuel engine based on RSM and NSGA-II. Energy Sources, Part A: Recovery, Utilization, and Environmental Effects, 45(4), 12503-12519. https://doi.org/10.1080/15567036.2023.2273406

https://doi.org/10.24191/jmeche.v23i1.8763